Available online at www.sciencedirect.com
ScienceDirect
Catalysis Today 122 (2007) 301–306
CATALYSIS TODAY
www.elsevier.com/locate/cattod

Catalytic oxidation of VOCs on Au/Ce-Ti-O

C. Gennequin, M. Lamallem, R. Cousin *, S. Siffert, F. Aïssi, A. Aboukaïs

Laboratoire de Catalyse et Environnement, E.A. 2598, Université du Littoral Côte d'Opale, 145 avenue Maurice Schumann, 59140 Dunkerque, France

Available online 19 April 2007

Abstract

$Ce_xTi_{1-x}O_2$ oxides have been synthesised by sol–gel method with x varying from 0 to 0.3 and characterised by XRD and TPR. The structure of oxides changes with the Ce/Ti molar ratio. The presence of ceria in Ce-Ti oxides inhibits the phase transition from anatase to rutile. When $x = 0.3$ ($Ce_{0.3}Ti_{0.7}O_2$ sample), the solid presents an amorphous state. The TPR results indicate that the presence of Ti enhances the reducibility of cerium oxide species. Catalytic oxidation of propene is investigated on Ce-Ti oxides and the better conversion is obtained with $Ce_{0.3}Ti_{0.7}O_2$ but the CO_2 selectivity reaches 63% at 400 °C. Gold is then deposited on theses oxides to improve the catalytic activity. On the basis of characterisation data (H_2 TPR), it has been suggested that gold influences the reduction of the Ce-Ti oxide support and the catalytic activity to the propene oxidation. Thus, Au/Ce-Ti-O system catalysts are promising catalysts for propene oxidation.

Keywords: Ceria; Titania; Gold; TPR; XRD; Propene oxidation

1. Introduction

Volatile organic compounds are recognised as major contributors to air pollution, either directly, through their toxic or malodorous nature, or indirectly, as ozone precursors. Many VOCs are health hazards in themselves and can cause cancer or other serious illnesses, even at low concentrations. Industrial processes and transportation activities are mainly responsible for the VOC emissions. Technologies for the removal of VOCs from gas streams can be broadly classified into two groups: those that recover the VOCs for possible later reuse and those that destroy the VOCs [1].

Catalytic oxidation of VOCs is a chemical process in which hydrocarbons are combined with oxygen at specific temperatures to yield carbon dioxide (CO_2) and water (H_2O). Catalytic oxidation is generally preferred to thermal combustion due to the lower temperature required and to its higher selectivity [2].

Gold has been until recently considered as one of the least catalytically useful metal because of its chemical inertness. However, in the last decade, it has been widely proved that it is possible to prepare gold nanoparticles deposited on metal oxide supports [3], which exhibit high catalytic activity towards oxidation reactions [4–13]. Supported gold catalyst on titania is often studied since its efficiency for the CO oxidation at low temperature are evidenced [4–10]. Moreover, gold supported on cerium oxide has been shown to possess high activity for VOC oxidation [14]. Ceria has been widely used in catalysis to purify vehicle exhausts and becomes the most rare earth oxide for controlling pollutant emission. It is known that ceria CeO_2 increases the dispersion of active components and its most important property is to serve as an oxygen reservoir which stores and releases oxygen via the redox shift between Ce^{4+} and Ce^{3+} under oxidizing and reducing conditions. The Ce^{3+}/Ce^{4+} redox cycle leads to high catalytic activity of CeO_2 [15–17]. However, since single CeO_2 would be sintered after calcinations at 750 °C, some mixed oxides are prepared by adding anti sintered oxides like titanium [18,19]. Thus, it should be interesting to combine the physicochemical properties of gold, titanium and cerium in order to obtain a suitable catalytic material for the total oxidation of VOCs.

In this work, we report a study of oxide supports containing titanium and cerium, which are prepared by a sol–gel method and treated at 600 °C under air. Samples are synthesised with different Ce and Ti molar ratios. These compounds are characterised by XRD, BET surface area and TPR techniques and tested in oxidation of propene, which is a probe molecule for VOCs oxidation. Then the aim of this work is to investigate

* Corresponding author. Tel.: +33 3 28 65 82 61; fax: +33 3 28 65 82 39.
E-mail address: cousin@univ-littoral.fr (R. Cousin).

0920-5861/$ – see front matter
doi:10.1016/j.cattod.2007.03.009

the role of gold and the support in the catalytic oxidation of propene.

2. Experimental

2.1. Preparation of Ce-Ti oxides and gold based catalysts

Titanium oxide sample (TiO_2) was prepared by sol–gel method. This method allows obtaining titanium oxide after calcination under air. The hydrolysis of titanium (IV) isopropoxide $Ti(OC_3H_7)_4$ with $H_2O/Ti(OC_3H_7)_4 = 5$ molar ratio diluted in an ethanol solution with molar ratio $Ti(OC_3H_7)_4/CH_3CH_2OH = 1/2$ was realised [20]. The gel obtained was dried at 80 °C during 24 h and finally calcined under air for 4 h at 600 °C to obtain titanium oxide powder (TiO_2).

$Ce_xTi_{1-x}O_2$ ($x = 0.1$–0.3) oxide samples were prepared by a sol–gel method [19,21]. An aqueous solution of cerium nitrate $Ce(NO_3)_3{\cdot}6H_2O$ and ethanol CH_3CH_2OH were added under stirring to another solution of ethanol CH_3CH_2OH and titanium (IV) isopropoxide $Ti(OC_3H_7)_4$ with molar ratio $Ti(OC_3H_7)_4/CH_3CH_2OH = 1/2$. The molar ratio between H_2O and titanium (IV) precursor is the same that for the titanium oxide preparation. The solution was gelled after finishing the reaction between titanium (IV) isopropoxide $Ti(OC_3H_7)_4$ and water. The gel was dried at 80 °C during 24 h and finally calcined under air for 4 h at 600 °C to obtain $Ce_xTi_{1-x}O_2$ oxides.

The gold-based catalysts (with a gold content of four weight percent) were prepared by the deposition precipitation (HDP) method [12]. Aqueous solution of tetrachloroauric acid ($HAuCl_4$) was added under stirring to an aqueous suspension of support with mixed oxides $Ce_xTi_{1-x}O_2$ calcined at 600 °C and aqueous solution of urea in excess. The solution is heated at 80 °C to decompose urea and obtain pH 6.7. In accordance with the literature data [12], the pH of solution was maintained at the value of 6.7 during 4 h to obtain high dispersion of fine gold particles on the oxide supports. The mixture was filtered and washed with deionised water at 60 °C several times in order to eliminate the chloride ions, dried during 24 h at 80 °C and finally calcined under air for 4 h at 400 °C.

2.2. Physico-chemical characterisation and catalytic test

XRD analysis was performed on a BRUKER Advance D8 powder X-ray diffractometer using Cu Kα radiation ($\lambda = 0.15406$ nm). Diffraction patterns were recorded over a 2θ range of 15–85° and using a step size of 0.02° and a step time of 4 s. The mean crystallite sizes were estimated using the Scherrer equation.

BET surface area was measured by nitrogen adsorption at −196 °C in an Ankersmit Quanta Sorb Junior apparatus. Before analysis, the samples were degassed for 30 min at 120 °C in vacuum.

To determine the elemental composition of samples, chemical analysis of Ce, Ti and Au was performed by inductively coupled plasma atomic emission spectroscopy at the CNRS Centre of Chemical Analysis (Vernaison, France).

The temperature programmed reduction experiments were carried out in an Altamira AMI-200 apparatus. The TPR profiles are obtained by passing a 5% H_2/Ar flow (30 mL/min) through 70 mg of samples heated at 5 °C/min from ambient temperature to 800 °C. The hydrogen concentration in the effluent was continuously monitored by a thermoconductivity detector (TCD).

Catalytic tests were carried out at atmospheric pressure in a continuous flow tubular glass reactor with an internal catalyst bed. A 100 mg quantity of the catalyst was loaded in the form of fine powder. The gas flow (100 mL/min with 6000 ppm propene in air) was controlled by mass flow controllers (qualiflow). The reactants and the reaction products were analysed by a VARIAN chromatograph (FID and TCD detector). The catalysts are first activated at 400 °C for 12 h and the conversion measurement is studied on heating ramp between 20 and 400 °C at 1 °C/min.

3. Results and discussion

3.1. Ce-Ti oxides study

Table 1 indicates the code name, the chemical composition and the evolution of specific surface areas of Ce-Ti oxides ($Ce_xTi_{1-x}O_2$ from $x = 0$ to 0.3) calcined under air at 600 °C. For titanium oxide TiO_2 sample, specific surface BET area is very low (3 m^2/g). When x value increases in $Ce_xTi_{1-x}O_2$ oxides, specific area increases to a maximum for $x = 0.3$ (86 m^2/g). This phenomenon can be explained by the adding of cerium during the preparation of the Ce-Ti oxides.

In order to determine the effect of cerium on the titania structure, XRD was performed. Fig. 1 shows the diffraction patterns of the oxides samples ($Ce_xTi_{1-x}O_2$ from $x = 0$ to 0.3) after calcination at 600 °C. The titanium oxide sample (TiO_2) is constituted by the anatase and rutile phases. These crystalline

Table 1
Code name, chemical composition, BET specific area of the Ce-Ti oxides and H_2-TPR consumption of oxides

Catalysts	Chemical composition[a]		Specific area (m^2/g)	H_2-TPR consumption (μmol/g)
Code name[a]	Experimental Ce content (molar ratio)	Experimental Ti content (molar ratio)		
TiO_2	0	1	3	–
$Ce_{0.1}Ti_{0.9}O_2$	0.090	0.909	50	502
$Ce_{0.2}Ti_{0.8}O_2$	0.208	0.791	66	984
$Ce_{0.3}Ti_{0.7}O_2$	0.300	0.699	86	1171

[a] The number after chemical symbol represents the atomic content obtained by chemical analysis in the solid.

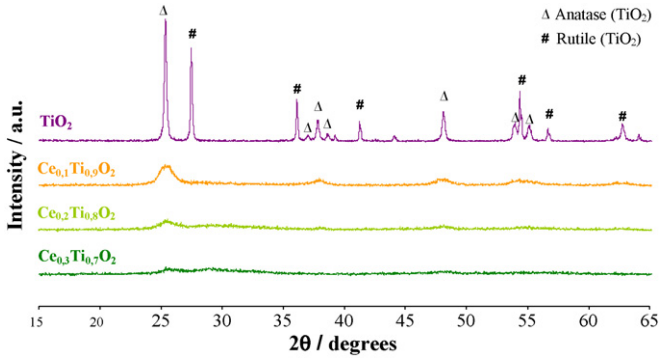

Fig. 1. XRD diagrams of Ce-Ti oxides calcined at 600 °C.

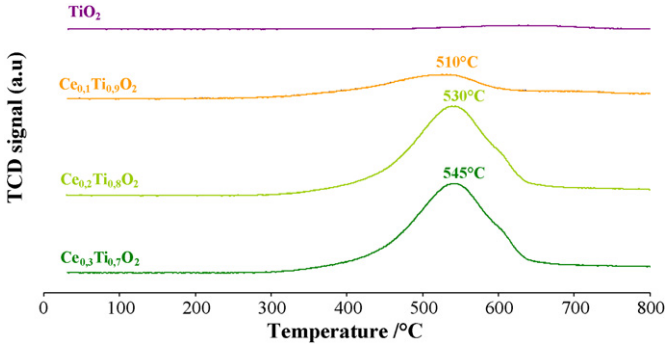

Fig. 2. TPR profiles of Ce-Ti oxides calcined at 600 °C.

phases are identified by comparing the recorded pattern with ICDD JCPDS files (anatase phase TiO_2 21–1272 and rutile phase TiO_2 21–1276). Theses phases are only observed for the TiO_2 sample. Courcot et al. [22] have calculated the percentage of rutile phase in the solid with the following formula: % rutile = $[1 - 1/(1 + 1.26I_R/I_A)] \times 100$, where I_R is rutile (1 1 0) diffraction peak intensity at $2\theta = 27.447^\circ$ and I_A is anatase (1 0 1) diffraction peak intensity at $2\theta = 25.281^\circ$ in diffractograms. Thus, in this work, titanium oxide sample contains 45% of rutile phase. The deeper crystallisation of titanium oxide (TiO_2) allows to explain the low specific area (3 m^2/g) obtained. For $Ce_xTi_{1-x}O_2$ samples (with $x = 0.1$–0.3), the crystalline structure of oxides changes with increasing Ce content in samples. The diffraction peaks of rutile phase disappear when a small amount of ceria is added and the crystalline structure of oxides consists only of TiO_2 anatase phase. According to the literature data [19], this result means that the addition of a small amount of ceria into titania inhibits the transition phase from anatase to rutile. It is interesting to note that the anatase phase can be stabilised in the presence of ceria because the rutile phase is known to be the most stable crystalline phase of titanium oxide. Anatase phase is detected in spite of the presence of ceria and the diffraction peaks become broader due to a lower crystallised state. For the $Ce_{0.3}Ti_{0.7}O_2$ compound, the XRD patterns exhibits very broad peaks due to amorphous state. This result is in accordance with the highest specific surface area obtained for the $Ce_{0.3}Ti_{0.7}O_2$ sample.

Fig. 2 shows the various profiles obtained after TPR measurements of the oxides. For titanium oxide sample, no significant reduction peak is detected in the temperature range from 20 to 800 °C. For the solids $Ce_xTi_{1-x}O_2$ with $x = 0.1$–0.3, respectively, a broad reduction peak is detected. This reduction peak shifts from 510 to 545 °C with increasing Ce content in binary oxides. In accordance with literature data [14,21], this reduction peak is generally attributed to reduction of oxygen species in the surface region of ceria. And, it is suggested that the presence of titania in sample facilitates the reduction of ceria surface oxygen species. Table 1 presents the H_2 consumption of Ce-Ti oxides. Supposing that only the CeO_2 component is reduced, it could be observed that H_2 consumption increases with increasing Ce content in mixed oxides. For comparison, the H_2 consumption of ceria synthesised in laboratory equals to 731 μmol/g correspond to a reduction degree of 25.1%. Thus, the H_2 consumption for Ce-Ti oxides compounds is much higher than that of pure ceria synthesised in laboratory. It is also reported in the literature [23] that the addition of TiO_2 in Ce-Ti-O system increased the reduction of CeO_2. It was shown that the presence of titania ions Ti^{4+} in Ce-Ti mixed oxides calcined at high temperature might weaken the Ce–O bond in the solid solution of mixed oxides and lead to an easier ceria reduction. Thus, the titanium enhances the reduction of ceria.

Fig. 3 shows the behaviour of $Ce_xTi_{1-x}O_2$ oxides (with $0 \leq x \leq 0.3$) as catalyst for propene oxidation. The propene conversion becomes measurable in the temperature range of 200–400 °C. With TiO_2 sample, the propene conversion is weak (<5% at 400 °C). When cerium is added to titanium to form binary oxide Ce-Ti, the propene conversion is better than titanium oxide. This improvement of conversion is due probably to the catalytic properties of CeO_2 present in the catalyst. The TPR results show the presence of CeO_2 on the surface of samples and the better reduction properties of Ce-Ti-O. The higher propene conversion is obtained with the $Ce_{0.3}Ti_{0.7}O_2$ sample, which previously presented the highest H_2 consumption. The conversion reaches 48% at 400 °C. The observed catalytic behaviour of $Ce_{0.3}Ti_{0.7}O_2$ could be thus related to the amorphous state. Indeed, the specific area of this compound is higher than other samples due to the amorphous state. More contact between the oxide and gas phase occurs during the propene oxidation. This good conversion result is also due to the presence of CeO_2 on the surface of these samples and to the effect of titanium on the ceria reduction. The redox

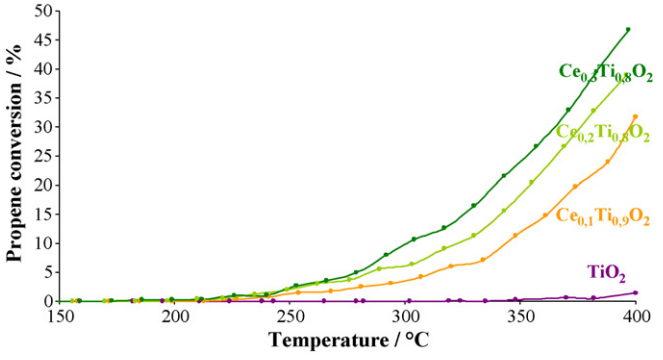

Fig. 3. Propene conversion vs. temperature over Ce-Ti oxides.

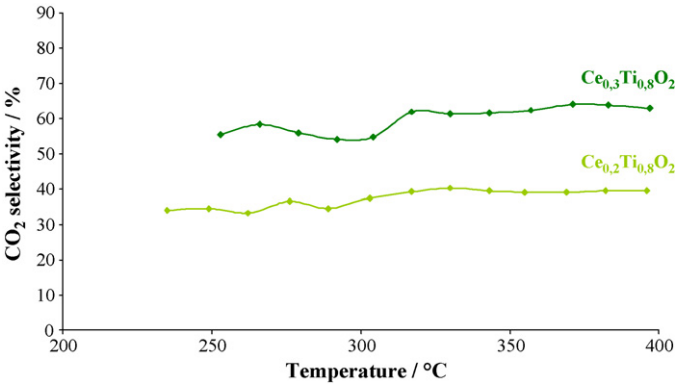

Fig. 4. CO_2 selectivity vs. temperature during propene conversion with $Ce_{0.2}Ti_{0.8}O_2$ and $Ce_{0.3}Ti_{0.7}O_2$ compounds.

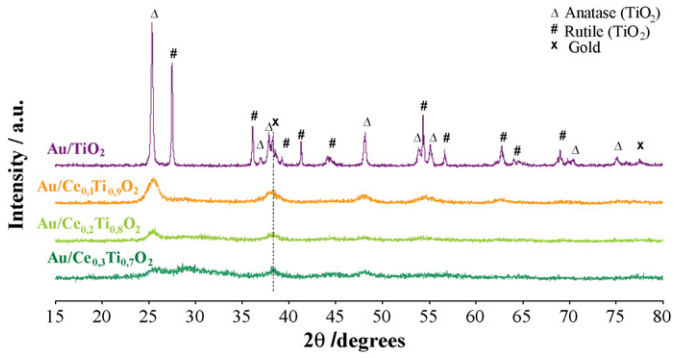

Fig. 5. XRD diagrams of gold on Ce-Ti oxides calcined at 400 °C.

properties of ceria can be claimed as one of those mainly responsible for this good conversion rate.

Concerning the selectivity some quantity of CO is formed with CO_2 during the propene oxidation by these oxides. Fig. 4 shows the CO_2 selectivity evolution as function of temperature of $Ce_xTi_{1-x}O_2$ oxides (with $x = 0.2$ and 0.3). The best selectivity into CO_2 is obtained for the $Ce_{0.3}Ti_{0.7}O_2$ solid. Whatever the temperature is, this catalyst leads to a formation of about 60% of carbon dioxide.

3.2. Gold deposited on Ce-Ti oxides

Gold is deposited on oxides as described in the experimental section. Fig. 5 reveals the XRD patterns for the gold-based catalysts. The XRD pattern for Au/TiO_2 sample presents besides the characteristic peaks of the structure of the TiO_2 support (anatase and rutile phases) the reflections due to the

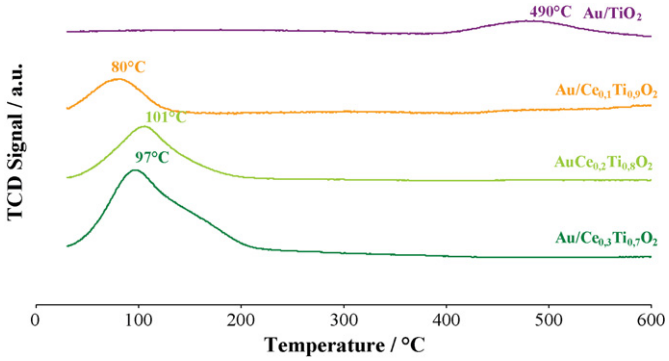

Fig. 6. TPR profiles of gold on Ce-Ti oxides calcined at 400 °C.

presence of gold (patterns at $2\theta = 38.2^\circ$ and 77.4°). These last peaks are identified by comparing with ICDD JCPDS file No. 04-0784. Gold metallic particles size has been deduced using Scherrer equation on the peak at 77.4° since at this angle no overlap with the rutile or anatase pattern of the support is observed. Thus, the gold particle size has been estimated at 40.9 nm. The percentage of rutile phase has been calculated and equal to 46%. This result is similar than the percentage value obtained for TiO_2 sample studied in this work. Thus, gold addition on the oxide support has no effect on the oxide support structure. For the samples $Au/Ce_xTi_{1-x}O_2$ (with $x = 0.1$–0.3, respectively), deposition of gold induces the appearance of small diffraction peaks of polycrystalline gold. The high amorphous character of the samples can be deduced from the high level of noise detected in the patterns. Only peak at 38.2° characteristic of Au° is discernable and is very weak and broad. After subtraction of the XRD pattern of the support, this peak emerges. The size of the gold crystallites, deduced from the broadening of this reflexion peak is between 6 and 7 nm for the $Au/Ce_xTi_{1-x}O_2$ samples (with $x = 0.1$–0.3, respectively). No change in the structure of the Ce-Ti-O support due to the introduction of gold is detected.

Table 2 reports the BET specific areas for the gold-based catalysts. The gold deposition procedure leads to a weakly modification of specific area. This table reveals also the experimental gold content in the solids and the H_2 consumption of the reduction peak at lower temperature. The TPR spectra of the gold deposited on mixed oxides are represented in Fig. 6. In the TPR spectrum of gold supported on titanium oxide TiO_2, a broad reduction peak is detected at 490 °C. This broad reduction peak is due to two overlapping peaks. One is attributed to the reduction of the oxygen species on the gold particles deposited on TiO_2 and the second is eventually

Table 2
Experimental gold content, BET surface areas and H_2-TPR consumption of gold-based catalysts

Catalysts code name	Experimental Au content (wt.%)	S_{BET} (m^2/g)	H_2-TPR total consumption (μmol/g)	Calculated H_2 consumption (μmol/g) for Au^{3+} into Au°	H_2 over consumption (μmol/g)
Au/TiO_2	3.22	3	587	244	343
$Au/Ce_{0.1}Ti_{0.9}O_2$	3.48	51	665	266	399
$Au/Ce_{0.2}Ti_{0.8}O_2$	2.67	65	717	205	512
$Au/Ce_{0.3}Ti_{0.7}O_2$	2.97	77	1195	228	967

attributed to the reduction of oxygen species TiO_2 support surface on the border with gold [24]. Table 2 resumes the H_2-TPR experimental and calculated consumption of catalysts samples for peaks at low temperature (<500 °C). For the H_2 calculated consumption, we consider that gold species are in the ionic state Au^{3+}. Thus, knowing the gold content in solids and following the reduction reaction of Au^{3+} into Au°, we can estimate a H_2 over consumption of the catalysts. The H_2 over consumption exists for gold deposited on TiO_2 but it is relatively weak compared with other compounds. This result shows the influence of gold to facilitate the reduction of oxygen species from TiO_2 support surface on the border with gold titanium oxide because without gold, the H_2 consumption for TiO_2 sample is very weak. Thus, a significant effect of gold on the reducibility of the titania surface oxygen is revealed. For gold deposited on Ce-Ti oxides (Fig. 6), a reduction peak at low temperature (between 80 and 101 °C) is revealed. This reduction peak of complex shape corresponding to two overlapping peaks is observed when Ce content increases in the sample ($Au/Ce_{0.3}Ti_{0.7}O_2$). For these compounds, the hydrogen consumption could arise from two processes which could be related to the reduction of oxygen species on different gold particles or/and to surface ceria oxygen species. The calculated H_2 consumption (Table 2) leads to hydrogen over consumption. Thus, gold on Ce-Ti oxides facilitates the reduction of surface oxygen species. The H_2 over consumption increases with an increase of cerium content to reach a maximum value for $Au/Ce_{0.3}Ti_{0.7}O_2$ sample. It is probable for this compounds that ceria is present in higher quantity on the surface than on the other solids. According to the results and literature data [14], the role of gold appears to modify the properties of ceria, enhancing the reducibility of CeO_2 surface oxygen species. It is probable that the presence of gold causes a decrease in the strength of the surface Ce–O bonds adjacent to gold atoms, thus leading to a higher surface lattice oxygen mobility and therefore to a higher reactivity of these oxygens.

The behaviour of gold deposited on $Ce_xTi_{1-x}O_2$ oxides (with $x = 0$–0.3) as a catalyst for propene oxidation is shown in Fig. 7. The conversion of propene becomes measurable in the range 200–400 °C and total selectivity to CO_2 is also found. We can observe that the presence of gold strongly enhances the rate of propene oxidation. Gold supported on Ce-Ti-O samples present considerably higher activities than supports alone. Catalytic

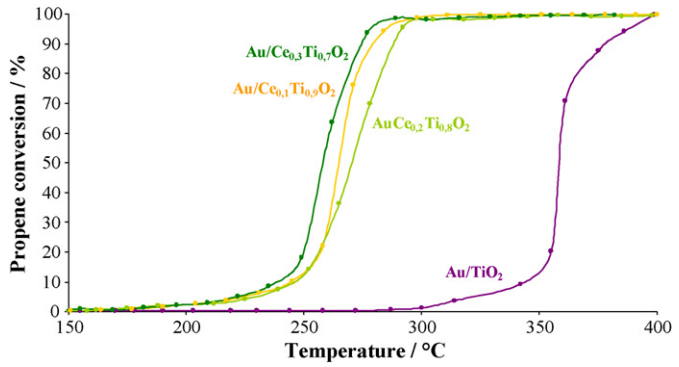

Fig. 7. Propene conversion into CO_2 vs. temperature over gold-based catalysts.

activity is strongly dependent on the chemical and physical nature of support. Au/TiO_2 sample is less active for propene oxidation. The dispersion of gold on support is an important factor to obtain high catalytic activity because high gold dispersion drives to obtain large number of specific catalytic sites for oxidation reaction. Titania oxide support presents a less specific surface area. The low surface area and the gold average crystallite size of 40.9 nm obtained for Au/TiO_2 compound can explain this catalytic result by a lower gold dispersion than other solids. When a small amount of cerium is added to TiO_2, catalytic activity is better than titania. This result is probably due to the ceria catalytic properties such as oxygen storage capacity. Moreover, ceria is known to promote the dispersion of active components [25]. The best result of propene conversion is obtained for gold deposited on $Ce_{0.3}Ti_{0.7}O_2$. In accordance with TPR results, the presence of gold modifying the properties of ceria enhances the reducibility of surface oxygen species. The reduction properties and the highest BET surface area of this compound could explain this catalytic result compared with the other compounds. Moreover, the XRD patterns of the Au/Ce-Ti-O show us small gold particle size. That is probably due to better dispersion of gold particles on the binary supports. This phenomenon can be caused by the effect of the adding of cerium in titania. Indeed, several authors [14,26,27] have shown that the oxygen mobility is an important factor to obtain higher oxidation activity. Sciré et al. [14] reveal that the high activity of Au/CeO_2 system in the field of VOCs oxidation might be related to the capacity of gold nanoparticles to weaken the Ce–O bond, thus increasing the mobility/reactivity of the surface lattice oxygen which is involved in the VOCs oxidation through a Mars-van Krevelen reaction mechanism. Moreover, Flytzani-Stephanopoulos and co-workers [27] have shown that gold nucleates probably at oxygen defect sites of ceria and remains highly dispersed and in good contact with the support for gold-ceria catalyst. Thus, the better catalytic activity of $Au/Ce_{0.3}Ti_{0.7}O_2$ catalyst is probably due to these interactions between gold and ceria.

4. Conclusion

Different solids $Ce_xTi_{1-x}O_2$ (with $0 \leq x \leq 0.3$) were prepared using sol–gel method. These compounds are characterised by XRD and H_2-TPR. The XRD study reveals that the crystalline structure of oxides changes when Ce content increases in binary oxides. At low cerium content, titania anatase phase is observed for $Ce_{0.1}Ti_{0.9}O_2$ and $Ce_{0.2}Ti_{0.8}O_2$ solids whereas the $Ce_{0.3}Ti_{0.7}O_2$ solid is amorphous. TPR of the Ce-Ti oxides shows that the reducibility of ceria is improved by the presence of Ti. Then, these oxides are tested in propene oxidation. Thus, the addition of cerium in titanium-based oxides enhances the propene conversion due to the catalytic properties of ceria. The better activity is obtained for $Ce_{0.3}Ti_{0.7}O_2$ sample but CO is formed during propene oxidation. Au/Ce-Ti-O solids were synthesised by deposition precipitation method using $HAuCl_4$ as precursor compounds. On the basis of the results reported, it can be concluded that

gold influences the reduction of the support. These latter compounds are very active towards propene oxidation and no CO is formed. The high activity is probably due to the ability of highly dispersed gold, which activate the oxygen of the Ce-Ti oxide weakening the Ce–Ti–O bonds located nearby the gold atoms. Therefore, gold deposited on Ce-Ti oxides are promising catalysts for propene oxidation.

Acknowledgements

The authors would like to thank the ''Conseil Général du Nord'', the ''Région Nord-Pas de Calais'' and the European Community (European Regional Development Fund) for financial supports.

References

[1] P. Le Cloirec, Les Composés Organiques Volatils (COV) dans l'Environnement, Lavoisier Tec&Doc, Paris, 1998.
[2] A. O'Malley, B.K. Hodnett, Catal. Today 54 (1999) 31.
[3] S. Ivanova, C. Petit, V. Pitchon, Appl. Catal. A 267 (2004) 191.
[4] G.C. Bond, Catal. Today 72 (2002) 5.
[5] R.J.H. Grisel, B.E. Nieuwenhuys, Catal. Today 64 (2001) 69.
[6] M. Daté, M. Haruta, J. Catal. 201 (2001) 221.
[7] M.A. Centeno, M. Paulis, M. Montes, J.A. Odriozola, Appl. Catal. A 234 (2002) 65.
[8] S. Minico, S. Sciré, C. Crisafulli, S. Galvagno, Appl. Catal. B 34 (2001) 277.
[9] J.D. Grundwaldt, M. Maciejewski, O.S. Becker, P. Fabrizioli, A. Baiker, J. Catal. 186 (1999) 458.
[10] M. Gasior, B. Grzybowska, K. Samson, M. Russel, J. Haber, Catal. Today 91–92 (2004) 131.
[11] R. Zanella, S. Giorgio, C.H. Shin, C.R. Henry, C. Louis, J. Catal. 222 (2004) 357.
[12] M. Haruta, Cattech 6 (2002) 102.
[13] R. Cousin, S. Ivanova, F. Ammari, C. Petit, V. Pitchon, in: Proceedings of the 2nd World Congress on Gold Applications, Vancouver, 2003.
[14] S. Sciré, S. Minico, C. Crisafulli, C. Satriano, A. Pistone, Appl. Catal. B 40 (2003) 43.
[15] S. Pengpanich, V. Meeyoo, T. Rirksomboon, K. Bunyakiat, Appl. Catal. A 234 (2002) 221.
[16] K. Otsuka, Y. Wang, M. Nakamura, Appl. Catal. A 183 (1999) 317.
[17] H.C. Yao, Y.F. Yu Yao, J. Catal. 86 (1984) 254.
[18] D. Terribile, A. Trovarelli, J. Llorca, J. Catal. 178 (1998) 299.
[19] J. Rynkowski, J. Farbotko, R. Touroude, L. Hilaire, Appl. Catal. A 203 (2000) 335.
[20] C. Pruvost, D. Courcot, E. Abi Aad, E.A. Zhilinskaya, A. Aboukaïs, J. Chim. Phys. 96 (1999) 1527.
[21] L. Mengfei, C. Jun, C. Linshen, L. Jiqing, F. Zhaochi, L. Can, Chem. Mater. 13 (2001) 197.
[22] D. Courcot, L. Gengembre, M. Guelton, Y. Barbaux, J. Chem. Soc. 90 (1994) 895.
[23] X. Jiang, L. Lou, Y. Chen, X. Zheng, Catal. Lett. 94 (2004) 49.
[24] V. Idakiev, Z.Y. Yuan, T. Tabakova, B.L. Su, Appl. Catal. A 281 (2005) 149.
[25] A. Trovarelli, C. Leitenburg, M. Boaro, Catal. Today 50 (1999) 353.
[26] D. Andreeva, P. Petrova, J.W. Sobczak, L. Ilieva, M. Abrashev, Appl. Catal. B 67 (2006) 237.
[27] M. Manzoli, F. Boccuzzi, A. Chiorino, F. Vindigni, W. Deng, M. Flytzani-Stephanopoulos, J. Catal. 245 (2007) 308.